



PUBLISHED BY INSTITUTE OF PHYSICS PUBLISHING AND SISSA

RECEIVED: August 10, 2007

ACCEPTED: September 21, 2007

PUBLISHED: October 1, 2007

GEM scintillation readout with avalanche photodiodes

**A.S. Conceição,^a L.F. Requicha Ferreira,^{a*} L.M.P. Fernandes,^a C.M.B. Monteiro,^a
L.C.C. Coelho,^a C.D.R. Azevedo,^{ab} J.F.C.A. Veloso,^{ab} J.A.M. Lopes^{ac} and
J.M.F. dos Santos^a**

^a *GIAN, Physics Dept., University of Coimbra,
P-3004-516 Coimbra, Portugal*

^b *Physics Department, University of Aveiro,
P-3810-193 Aveiro, Portugal*

^c *Instituto Superior de Engenharia de Coimbra,
Apartado 4065, P-3030-199 Coimbra, Portugal
E-mail: requicha@ci.uc.pt*

ABSTRACT: The use of the scintillation produced in the charge avalanches in GEM holes as signal amplification and readout is investigated for xenon. A VUV-sensitive avalanche photodiode has been used as photosensor. Detector gains of about 4×10^4 are achieved in scintillation readout mode, for GEM voltages of 490 V and for a photosensor gain of 150. Those gains are more than one order of magnitude larger than what is obtained using charge readout. In addition, the energy resolutions achieved with the scintillation readout are lower than those achieved with charge readout. The GEM scintillation yield in xenon was measured as a function of GEM voltage, presenting values that are about a half of those achieved for the charge yield, and reach about 730 photons per primary electron at GEM voltages of 490 V.

KEYWORDS: Gaseous detectors; Electron multipliers (gas); Hybrid detectors.

* Corresponding author.

Contents

1. Introduction	1
2. Experimental set-up and method	2
3. Experimental results and discussion	4
3.1 Comparison between charge and scintillation readout modes	4
3.2 GEM scintillation yield in xenon at atmospheric pressure	5
4. Conclusions	6

1. Introduction

The use of the scintillation produced in electron avalanches has been an alternative for signal amplification and readout in radiation detectors. In opposition to conventional electronic readout of avalanche charge, the optical readout of avalanche scintillation results in a fast propagating pulse, insensitive to electronic noise, RF pick-up and high-voltage problems, since the readout is electrically decoupled from the signal amplifying elements. Time projection chambers (TPCs) with optical readout have been developed [1],[2], but only few applications to radiation detection [3]-[6] and to nuclear physics experiments [7],[8] have been implemented.

Pure noble gases and CF_4 exhibit the highest scintillation yields but, on the other hand, scintillate in the VUV region ($\lambda < 200$ nm). This feature inhibits their use as high-gain counting gases in most gaseous detectors, due to photon-mediated feedback effects that usually limit the detector's gain and performance. This drawback was overcome with the introduction of the Gas Electron Multiplier (GEM) [9]. The avalanche confinement within the GEM holes effectively hinders photon-mediated secondary processes, allowing high gains to be achieved in highly UV-scintillating gases [10],[11].

The first studies investigating the scintillation produced in GEM avalanches were described in [4]-[6] and references therein. They used gas mixtures scintillating in the visible range and a highly sensitive CCD camera readout for imaging. This system presents a very good 2D-position resolution but, on the other hand, is limited by the intrinsic slow response capability of the CCD for charge readout.

In this work we investigate the performance characteristics of GEM scintillation in pure xenon using a VUV-sensitive large area avalanche photodiode (LAAPD) as the photon readout. The amplitude and energy resolution of the scintillation pulse-height distributions are determined as a function of GEM voltage and compared to those of charge pulses. The xenon scintillation yield obtained in GEMs is measured as a function of GEM voltage.

Xenon presents the highest scintillation yield and is of particular interest for application in direct dark matter search experiments (XENON [12] and ZEPLIN [13]), which use dual-phase xenon TPCs with secondary scintillation production and readout in the gas phase. Both scintillation in the liquid and in the gas phase are detected by means of PMTs. XENON has the

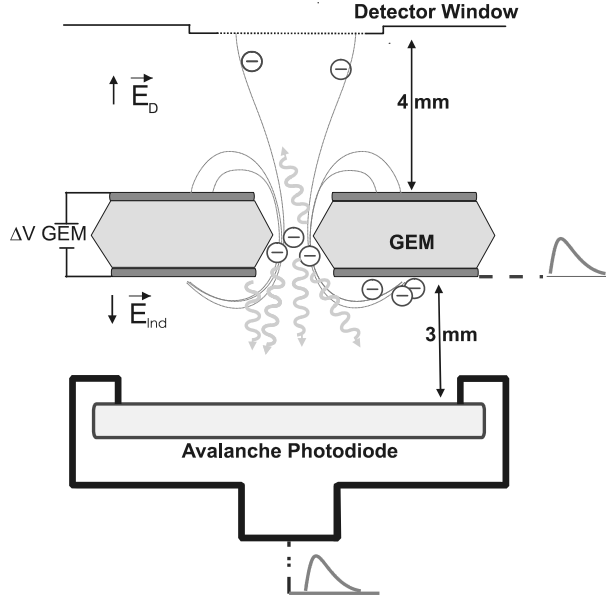


Figure 1. Schematic diagram of the single-GEM with LAAPD scintillation readout used in this work.

best sensitivity reached thus far for WIMP detection [14]. The largest source of background in the XENON detector is the radioactivity of the PMT glass and of the stainless steel detector body. The sensitivity of the detectors applied to dark matter search will be limited by this radioactivity and alternatives to PMTs are under investigation, e.g. [15],[16].

Avalanche photodiodes (APDs) are good candidates for the GEM scintillation readout, for they are compact and present low-power consumption, high quantum efficiency and insensitiveness to intense magnetic fields. In addition, the relatively low response to ionising particles make them competitive for the use in medium and high-energy physics instrumentation, being good alternatives to photomultipliers in visible- and VUV-photon detection [17],[18]. In particular, their negligible radioactivity contamination is attractive for low background experiments, such as direct dark matter search. On the other hand, their low gain and reduced active area present the main drawbacks when compared to PMTs.

2. Experimental set-up and method

The GEMs used in this work were manufactured at CERN and have standard dimensions: 50 μm Kapton with 5 μm copper clad on both sides and bi-conical holes of 50 and 70 μm in the Kapton and copper, respectively, arranged in a hexagonal layout of 140 μm edges. The GEMs active area is $2.8 \times 2.8 \text{ cm}^2$. A stainless-steel detector body was built to accommodate both GEM and LAAPD, figure 1. The GEM is mounted on a Macor frame, which keeps the former stretched and provides the electrical contacts to the GEM surfaces. Macor pieces, glued to the stainless-steel body with low vapour-pressure epoxy (Tra-Con 2116), are used for insulating the feedthroughs of the GEM biasing. The LAAPD is vacuum tight by compression of an indium gasket against the detector body. The detector window is made of aluminized Mylar foil (25 μm thick) glued to the detector body with the above mentioned epoxy.

The detector was pumped down to pressures below 10^{-5} mbar, filled with xenon at 1 atm and sealed off during the measurements. The gas purity was maintained using non-evaporable getters (SAES St707), heated up to about 120°C and placed in a small volume connected to the detector. The LAAPD enclosure and the detector body were grounded, while the detector

window, GEM top and bottom electrodes were polarized independently. The voltage difference between detector window and GEM top electrode determines the drift field, E_D ; the voltage difference between GEM top and bottom electrodes, ΔV_{GEM} , determines the avalanche gain in the holes; the voltage in the GEM bottom electrode determines the induction field, E_{Ind} . Constant drift and induction fields of 0.5 and -0.1 kV/cm, respectively, and LAAPD bias voltage of 1840 V were used throughout the measurements.

The detector was irradiated with a 1 mm collimated x-ray beam from a ^{109}Cd source, providing a clear separation of the peak distribution from the electronic noise tails, for reduced detector gains. The primary electron cloud resulting from x-ray interaction in the drift region is focused into the holes where they undergo avalanche multiplication, figure 1. The avalanche electrons are extracted out of the holes and collected in the GEM bottom. A large number of scintillation photons ($\lambda \sim 172$ nm) are also produced in the charge avalanche, as a result of the gas de-excitation processes. A fraction of these photons will reach the LAAPD active-area, and the corresponding electric signal is amplified through charge-avalanche processes in the photodiode. As for the avalanche electrons, the number of scintillation photons is proportional to the number of primary electrons and, thus, to the x-ray energy.

The signals from both GEM bottom and LAAPD were fed through two independent electronic chains, consisting of a Canberra 2006 preamplifier (1.5 V/pC sensitivity) and a Hewlett Packard 5582A linear amplifier (2 μs integration and differentiation shaping time constants) and a Nucleus PCA II 1024-multichannel analyser (MCA). The sensitivities of both chains were calibrated for absolute gain determination. For this purpose, a calibrated capacitor was directly connected to the preamplifier input as well as to a precision pulse generator. The gains were determined from the peak position of the pulse-height distributions.

The direct interactions of the 22.1 keV x-rays in the LAAPD can be used as a reference for determining the absolute number of VUV-photons impinging the LAAPD. While the amplitude of the scintillation pulses depends on both GEM voltage and LAAPD biasing, the amplitude of the events resulting from direct x-ray interactions in the LAAPD depends only on the LAAPD biasing. In addition, the latter pulses are present even for null biasing voltages in the GEM and in the absorption and induction regions. A direct comparison between the amplitudes of the pulses resulting from scintillation and x-rays fully absorbed in the APD provides a direct quantification of the VUV-photons impinging the LAAPD, given the quantum efficiency of the device. This method has been largely employed to measure the primary scintillation yield of inorganic crystals, e.g. [19] and references therein, and the electroluminescence yield of pure xenon in uniform electric fields [20].

Typical pulse-height distributions obtained for ^{109}Cd x-rays are depicted in figure 2 a) and b) for charge and scintillation signal readout modes, respectively. The spectral features include the Ag K-lines, Cu and Fe fluorescence K-lines resulting from ^{109}Cd x-ray interaction in the GEM copper layers and in the stainless steel meshes used to support the Mylar window, the xenon L-fluorescence-escape peaks and the electronic noise tail in the low-energy limit. The pulse height distributions resulting from the direct interaction of the x-rays in the APD are superimposed on the noise tail and are not visible.

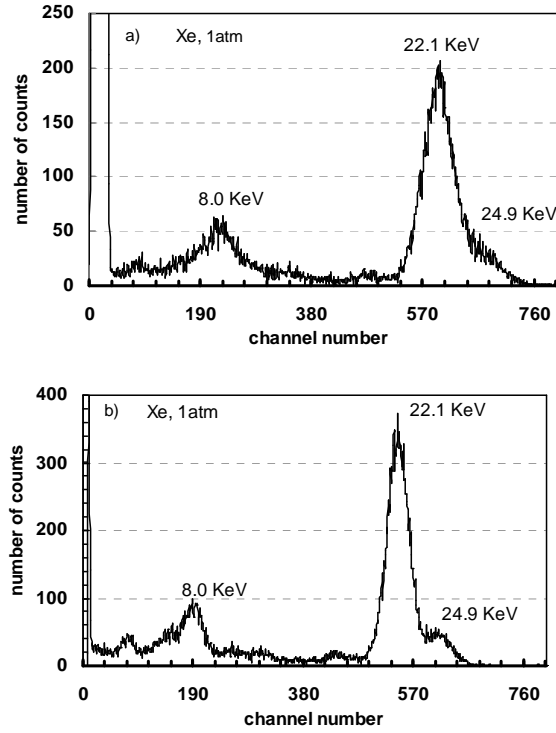


Figure 2. Pulse-height distributions obtained with the GEM detector instrumented with a large-area APD for ^{109}Cd x-rays: (a) charge and (b) scintillation readout modes. $\Delta V_{\text{GEM}} = 480$ V.

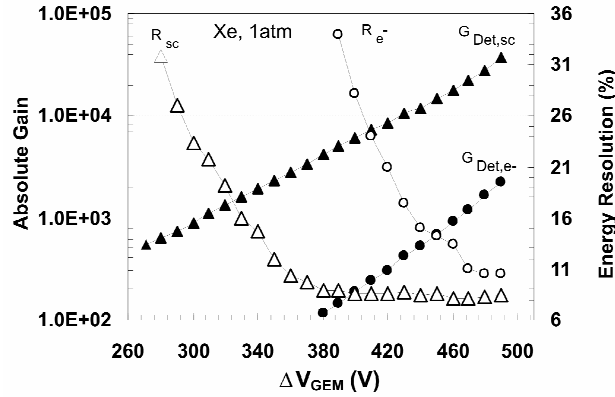


Figure 3. Detector total gain and energy resolution as a function of voltage difference applied across the GEM holes, ΔV_{GEM} , for 22.1 keV x-rays, and for scintillation and charge signal readout modes.

3. Experimental results and discussion

3.1 Comparison between charge and scintillation readout modes

Figure 3 depicts the absolute detector gain and energy resolution for 22.1 keV x-rays obtained in charge and scintillation readout modes, as a function of GEM voltage. ΔV_{GEM} was gradually increased, up to the onset of micro-discharges. The gains achieved through scintillation readout are more than one order of magnitude higher than those achieved using charge readout. Gains of about 4×10^4 and 2×10^3 , respectively, are reached at the maximum GEM voltage of 490 V. In

addition, the detector energy resolution is lower for scintillation readout, being about 9% for GEM voltages as low as 380 V and decreasing slowly down to about 8% for the highest GEM voltages. For charge readout mode, the detector energy resolution is about 10% for GEM voltages of 490 V, degrading rapidly as ΔV_{GEM} decreases.

We demonstrated that, using the scintillation as signal readout, it is possible to achieve high gains and good energy resolutions with single-GEM in xenon, even for low GEM voltages, allowing very stable operation with reduced discharge probability. For example, a gain of 10^4 is obtained at a GEM voltage of 430 V, 25 times higher than the corresponding gain obtained with charge readout. For these conditions, the detector energy resolution for 22.1 keV x-rays is 9 and 18% in scintillation and charge readout mode, respectively.

We note that, in this work, the avalanche electrons are collected in the GEM bottom-electrode. In practical cases, the effective gain of the GEM is associated with the charge collected in the induction plane and depends on the induction field. At atmospheric pressure, induction fields as high as 3 kVcm^{-1} result in electron collection efficiencies around 50% [21], i.e. in an effective gain that is a half of the total gain achieved in GEM holes, depicted in figure 3.

3.2 GEM scintillation yield in xenon at atmospheric pressure

The pulse amplitude resulting from 22.1 keV x-ray full-absorption in the APD was obtained from the respective pulse-height distribution taken for null electric fields in the drift and induction regions and null GEM voltage, and for an APD bias voltage of 1840 V. This amplitude was corrected for APD gain non-linearity effects present in x-ray detection [19].

The ratio between the amplitude of the scintillation pulses resulting from the 22.1 keV full absorption in the gas, e.g. in figure 2, and the amplitude resulting from the direct interaction of the x-rays in the APD, $A_{\text{UV}}/A_{\text{RX}}$, provides a direct measurement of the number of charge carriers, $N_{e,sc}$, produced in the photodiode by the scintillation pulse:

$$N_{e,sc} = N_{e,XR} \times \frac{A_{\text{UV}}}{A_{\text{XR}}} \quad (3.1)$$

where $N_{e,XR}$ is the number of charge carriers produced in the APD resulting from 22.1 keV x-ray full absorption;

$$N_{e,XR} = \frac{22.104 \text{ keV}}{3.62 \text{ eV}} \cong 6.1 \times 10^3 \text{ free electrons} \quad (3.2)$$

as the w -value in silicon is 3.62 eV [22].

A direct quantification of the VUV-photons produced in the GEM holes, N_{UV} , is obtained given the quantum efficiency of the device, QE , and the solid angle subtended by the APD, relative to the scintillation region, Ω_{sc} :

$$N_{\text{UV}} = \frac{N_{e,sc}}{QE} \times \frac{4\pi}{\Omega_{sc}} = \frac{A_{\text{UV}}}{A_{\text{XR}}} \times \frac{N_{e,XR}}{QE} \times \frac{4\pi}{\Omega_{sc}} \quad (3.3)$$

A value of $QE = 1.1$ for the number of charge carriers produced in the photodiode per incident 172 nm VUV photon was provided by the manufacturer [23] for the LAAPDs we used. The average solid angle subtended by the APD is obtained assuming that the scintillation occurs at the detector axis, 3 mm away from the 16 mm diameter APD. Therefore, $\Omega_{sc}/4\pi = 0.32$.

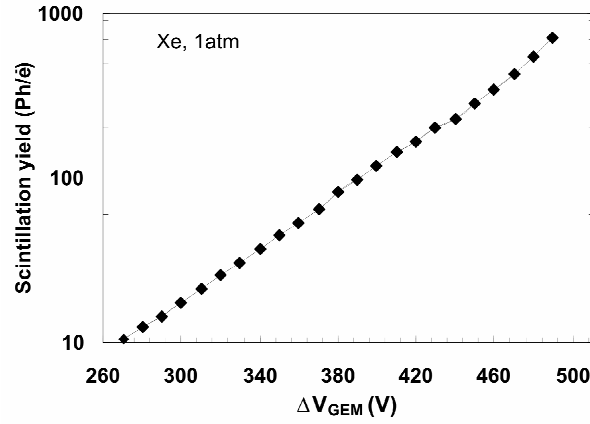


Figure 4. Scintillation yield, i.e. number of photons produced per primary electron in the GEM holes, as a function of voltage difference applied across the GEM holes, ΔV_{GEM} , for xenon at 1 atm.

The GEM scintillation yield, Y , i.e. the number of photons produced in the GEM holes per primary electron, is given by

$$Y = N_{UV} \left(\frac{22.104 \text{ keV}}{21.77 \text{ eV}} \right)^{-1} \quad (3.4)$$

considering a w -value for xenon of 21.77 eV for 22.1 keV x-rays [24].

Figure 4 depicts the GEM scintillation yield in xenon at 1 atm as a function of GEM voltage. The number of photons produced in electron avalanches in the GEM holes is about a half of the number of avalanche electrons, reaching about 730 photons per primary electron at GEM voltages of 490 V. However, the additional gain and the lesser statistical fluctuations associated with the scintillation detection and amplification in the photosensor, when compared to those associated with the charge-avalanche amplification, is an advantage of the scintillation readout mode.

The GEM scintillation yield reached for a GEM voltage of 470 V is similar to that obtained for the electroluminescence produced in a 1 cm drift scintillation region and a uniform field of $4 \text{ kVcm}^{-1}\text{bar}^{-1}$ in a GPSC [20]. On the other hand, the GEM scintillation yield achieved in xenon is 3 orders of magnitude larger than reached in quenched mixtures, e.g. [8].

We can write the detector gain for the scintillation readout mode as

$$G_{\text{Det},sc} = N_{e,sc} G_{\text{APD}} \left(\frac{22.104 \text{ keV}}{21.77 \text{ eV}} \right)^{-1} \quad (3.5)$$

where $G_{\text{Det},sc}$ is the absolute detector gain presented in figure 3 for the scintillation readout mode and $N_{e,sc}$ is obtained from eq. (3.1). Therefore, our results are consistent with an APD gain, G_{APD} of about 150, at 1840 V, a value that is in good agreement with our APD gain measurements using x-rays and with the manufacturer data sheet. This gain can still be increased by a factor of two, increasing the LAAPD biasing voltage.

4. Conclusions

We have investigated the performance achieved with a single-GEM operated in pure xenon at atmospheric pressure, when reading the scintillation pulses produced in charge avalanches. An avalanche photodiode with high quantum efficiency in the VUV region was used for scintillation

readout. The maximum gain achieved prior to the onset of micro-discharges is about 4×10^4 at a GEM voltage of 490 V, while a gain of about 10^4 is achieved at a GEM voltage of 430 V, a factor of about 50 higher when compared to the avalanche charge readout in the induction plane. In addition, the energy resolution achieved with scintillation readout is better than that achieved with charge readout, being 8 and 10%, respectively, for 22.1 keV x-rays and for the highest gains. For charge readout, the detector energy resolution degrades rapidly for GEM voltages below 470 V, while for scintillation readout this happens only for voltages below 380 V.

The scintillation yield achieved in GEMs was measured as a function of GEM voltage and yields of about 730 and 200 photons per primary electron were measured at GEM voltages of 490 and 430 V, respectively. These values are about a half of those achieved for the GEM avalanche electrons. Nevertheless, for GEM voltages above 470 V, the GEM scintillation yield is higher than that obtained for a xenon gas scintillation counter with a $4 \text{ kV cm}^{-1} \text{ bar}^{-1}$ uniform field, 1 cm thick scintillation region.

We have demonstrated that the GEM-APD scintillation readout is a good alternative to the standard stainless steel double mesh-PMT readout for reduced background in direct dark matter search experiments such as XENON and ZEPLIN. The cost of VUV-sensitive APDs can be a drawback but, in recent years, efforts have been made to develop low-cost, large-area APDs with sensitivity below 200 nm and high quantum efficiency.

Future work will include the study of the performance characteristics of GEM scintillation in xenon at higher pressures. As the gas excitation is the alternative process to gas ionisation in electron avalanches, the scintillation readout present a behaviour that is different from the fast gain decrease with pressure, in opposition to the charge avalanche gain. In THGEMs, the scintillation readout is expected to be even more favourable, when compared to charge readout, since the electric fields achieved in THGEM are lower than those achieved in GEM, favouring the gas excitation processes.

Acknowledgements

Support is acknowledged to FEDER and Fundação para a Ciência e a Tecnologia (FCT, Portugal), through Project PTDC/FIS/65121/06. C.M.B. Monteiro acknowledges PhD Grant SFRH/BD/25569/05.

References

- [1] A. Breskin et al., *A highly efficient low-pressure UV-rich detector with optical avalanche recording*, *Nucl. Instrum. Meth. A* **273** (1988) 798.
- [2] P. Fonte, A. Breskin, G. Charpak, W. Dominik and F. Sauli, *Beam test of an imaging high-density projection chamber*, *Nucl. Instrum. Meth. A* **283** (1989) 658.
- [3] U. Titt et al., *A time projection chamber with optical readout for charged particle track structure imaging*, *Nucl. Instrum. Meth. A* **416** (1998) 85.
- [4] F.A.F. Fraga et al., *Optical readout of GEMs*, *Nucl. Instrum. Meth. A* **471** (2001) 125.
- [5] S. Fetal et al., *Dose imaging in radiotherapy with an Ar-CF₄ filled scintillating GEM*, *Nucl. Instrum. Meth. A* **513** (2003) 42.
- [6] G. Manzin, B. Guerard, F.A.F. Fraga and L.M.S. Margato, *A gas proportional scintillator counter for thermal neutrons instrumentation*, *Nucl. Instrum. Meth. A* **535** (2004) 102.

- [7] M. Cwiok et al., *Optical time projection chamber for imaging of two-proton decay of ^{45}Fe nucleus*, *IEEE Nucl. Sci. Symp. Conf. Rec.* **2** (2004) 1152.
- [8] L. Weissman et al., *Amplification and scintillation properties of oxygen-rich gas mixtures for optical-TPC applications*, *JINST* **1** (2006) P05002.
- [9] F. Sauli, *GEM: A new concept for electron amplification in gas detectors*, *Nucl. Instrum. Meth. A* **386** (1997) 531.
- [10] A. Buzulutskov et al., *GEM operation in pure noble gases and the avalanche confinement*, *Nucl. Instrum. Meth. A* **433** (1999) 471.
- [11] A. Breskin, A. Buzulutskov and R. Chechik, *GEM photomultiplier operation in CF_4* , *Nucl. Instrum. Meth. A* **483** (2002) 670.
- [12] E. Aprile et al., *The XENON dark matter search experiment*, *New Astron. Rev.* **49** (2005) 289.
- [13] D.Yu. Akimov et al., *The ZEPLIN-III dark matter detector: Instrument design, manufacture and commissioning*, *Astropart. Phys.* **27** (2007) 46.
- [14] J. Angle et al., *First results from the XENON10 dark matter experiment at the Gran Sasso National Laboratory*, accepted for publication in *Phys. Rev. Lett.* (2007).
- [15] M.Gai et al., *Toward application of a Thick Gas Electron Multiplier (THGEM) readout for a dark matter detector*, Proc. 23rd Winter Workshop on Nuclear Dynamics, Big Sky, Montana, Feb. 11-18, 2007, arXiv:0706.1106v1.
- [16] L.M.P. Fernandes, E. Aprile, K.L. Giboni, J.A.M. Lopes and J.M.F. dos Santos, *Operation of avalanche photodiodes in liquid xenon*, submitted for publication to *Nucl. Instrum. Meth. A*.
- [17] M. Moszynski, M. Szawlowski, M. Kapusta and M. Balcerzyk, *Avalanche photodiodes in scintillation detection*, *Nucl. Instrum. Meth. A* **497** (2003) 226.
- [18] C.M.B. Monteiro, L.M.P. Fernandes, J.A.M. Lopes, J.F.C.A. Veloso and J.M.F. dos Santos, *Detection of VUV photons with large-area avalanche photodiodes*, *Appl. Phys.* **B 81** (2005) 531.
- [19] M. Moszynski, M. Szawlowski, M. Kapusta and M. Balcerzyk, *Large area avalanche photodiodes in scintillation and X-rays detection*, *Nucl. Instrum. Meth. A* **485** (2002) 504.
- [20] C.M.B. Monteiro et al., *Secondary scintillation yield in pure xenon*, *JINST* **2** (2007) P05001.
- [21] F.D. Amaro et al., *Operation of a single-GEM in noble gases at high pressures*, *Nucl. Instrum. Meth. A* **579** (2007) 62.
- [22] G.F. Knoll, *Radiation detection and measurement*, 3rd Edition, Wiley, New York U.S.A. (2000).
- [23] B. Zhou and M. Szawlowski, *An explanation on the APD spectral quantum efficiency in the deep UV range*, Interoffice Memo, Advanced Photonix Inc., 1240 Avenida Acaso, Camarillo, CA 93012, EUA (1999).
- [24] T.H.V.T. Dias et al., *Full-energy absorption of x-ray energies near the Xe L- and K-photoionization thresholds in xenon gas detectors: simulation and experimental results*, *J. Appl. Phys.* **82** (1997) 2742.